SPARSE ARRAY OF THERMAL RESONATORS FOR INFRARED DETECTION AND IMAGING

Isabel H. Rodrigues[1], Clifford F. Frez[1], Savannah R. Eisner[2,3], Debbie G. Senesky[2], and Mina Rais-Zadeh[1]
[1]Jet Propulsion Laboratory, California Institute of Technology, USA,
[2]Stanford University, USA, [3]Columbia University, USA

ABSTRACT

Exploring extreme environments in our solar system, such as like Venus or Mercury, poses significant challenges due to high temperatures and corrosive atmospheres. Current technology struggles in such conditions, limiting payload endurance. This study introduces an infrared (IR) imaging device with micromechanical resonant sensors, tailored for extreme environments (>400°C). It captures IR radiation and translates it into heat, showcasing unprecedented resilience and accurate IR power measurement. The sparse array efficiently routes signals without sacrificing imaging resolution. Fabrication employs metal-organic chemical vapor deposition and GaN-on-Si MEMS processes, ensuring stability up to 500°C. High-quality performance is demonstrated through RF measurements, paving the way for future planetary exploration and remote sensing.

KEYWORDS

Detector, harsh environment, high-temperature measurement infrared sensors, sparse array, thermal IR.

INTRODUCTION

The exploration of the extreme environments within our solar system presents monumental challenges that stem from the intensely high temperatures and corrosive atmospheres prevalent in these locales. Over the course of history, spacecraft and probes dispatched to these distant destinations have endured only fleetingly, largely due to the inherent limitations of the sensors and electronics they carry. Existing technology often falters in the face of such extreme conditions, as the majority of sensors and their associated readout electronics are not capable of functioning beyond specific thermal thresholds, thresholds that are easily surpassed on these hostile planets. Studying unforgiving surfaces of planetary bodies, such as Venus – often dubbed Earth's twin due to shared characteristics like size, mass, composition, and weather – can offer insights into our own environment's geology and climate dynamics. Infrared (IR) imaging is crucial for understanding Venus's surface, where temperatures reach 475°C and blackbody radiation peaks at 4 µm. This work aims to address these challenges by developing an IR imaging instrument utilizing a sparse array of resonant-based micromechanical devices, leveraging previously characterized GaN resonators [1].

The resonant pixels absorb incoming IR radiation via a high-temperature-tolerant IR absorber, translating it into heat. The resonant frequency changes with increased temperature following the temperature coefficient of frequency (TCF) characteristic of the device and agnostic to its base temperature, ensuring robust operation over a wide temperature range, unlike existing solutions vulnerable to saturation at 100-300°C.

Heterogenous integration of sensors and readout electronics presents challenges at high temperatures due to increased stress and thermal issues, necessitating their monolithic integration on the same chip. InAlN/GaN transistors, functional at temperatures up to 1000°C, offer a viable solution [2]. While monolithic integration ensures stability, signal routing from each pixel to electronics consumes chip area, reducing image resolution. The sparse array architecture presented in this work (Fig. 1) facilitates signal routing, simplifying integration and packaging of the IR detector, reducing complexity, and power consumption. In a sparse array configuration, the number of imaging elements is intentionally reduced to conserve power and lower costs, a methodology commonly employed in medical imaging instruments for constructing 3D images from low-power 2D arrays, albeit with added processing time and modest post-processing power [3]-[10].

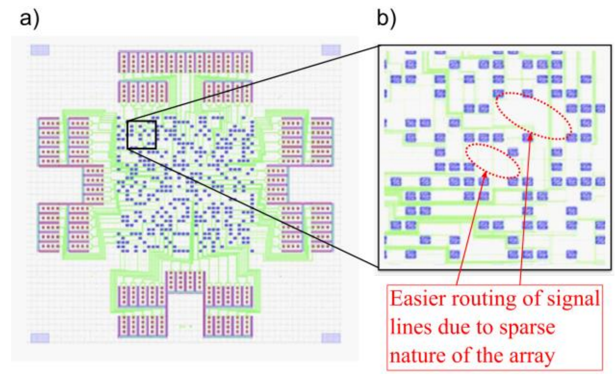

Figure 1: (a) Sparse array design with 384 resonant pixels, and (b) a zoomed in area illustrating the easier routing of signal lines due to sparse nature of the array.

Our sparse array is engineered to withstand and operate effectively in environments characterized by soaring temperatures reaching up to 500°C. The study showcases the unparalleled resilience of this sensor in enduring extreme heat while accurately measuring IR power, promising diverse applications ranging from imaging planetary surfaces like Venus to the potential for broader-scale imaging endeavors.

Sparse array structure and image recovery aspects of this IR imaging system have been published previously [1], where random sparse arrays were constructed and used in conjunction with the Compressed Sensing (CS) concept to reconstruct accurate images. This paper presents measured results on the IR performance of both the sparse and a dense array of resonators that would be able to operate in harsh space environments and bring science returns usable in the mentioned CS concept.

DESIGN AND FABRICATION

The sparse array design is meticulously crafted to ensure minimal loss in overall imaging resolution while routing signals from each pixel (resonator) to integrated electronics. Fig. 1 (b) shows a close-up of the sparse array design illustrating easier routing of signal lines due to the sparse nature of the array.

Fabrication of this thermal imaging array (Fig. 2) employs a metal-organic chemical vapor deposition technique for the growth of InAlN/GaN or AlGaN/GaN epitaxial layers, complemented by well-established GaN-on-Si MEMS processes tailored specifically for harsh environments [11], [12]. The device layered architecture consists of stacks of InAlN(or AlGaN)/AlN/GaN/AlN with

978-1-940470-05-4/HH2024/$25©2024TRF
DOI 10.31438/TRF.HH2024.58

Solid-State Sensors, Actuators, and Microsystems Workshop
Hilton Head Island, South Carolina, 2-6 June 2024

specified thicknesses of 2 nm/ 15 nm/ 1 nm/ 550 nm/ 80 nm, all built atop silicon (111) wafers procured from NTT Japan. The isolation of each device is achieved through a mesa-etch process. Ohmic contacts comprised of a Ti/Al/Pt/Au stack (10 nm/ 100 nm/ 40 nm/ 80 nm) deposited via electron beam evaporation, lifted off, and annealed for 30 s in N_2 at 850°C. This metallization scheme [13] has demonstrated stability at 600°C on GaN and was employed for creating metal interconnects to the InAlN/GaN-on-silicon devices. The top AlGaN (or InAlN) was then removed from the resonating area and Schottky contacts were deposited. The absorber layer was then deposited and patterned. The nominal device consists of a plasmonic absorber with a peak absorption wavelength of 4 µm. The prototype, reported in this paper, consisted of a 50 nm thick silicon nitride absorber. The devices then underwent dry release using silicon deep reactive ion etching from the backside. Variants of this process have recently facilitated the realization of high-temperature tolerant GaN resonators for missions to Venus [14].

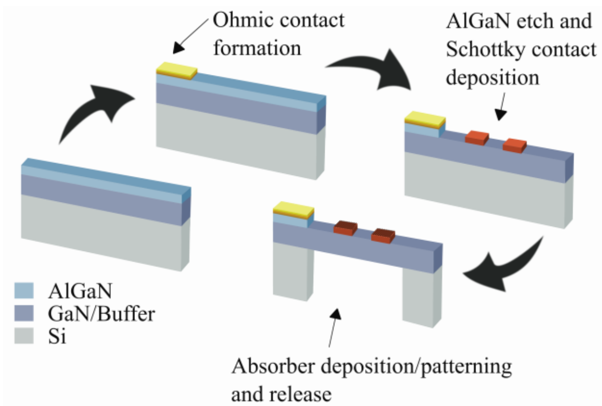

Figure 2: Schematic of the main fabrication process steps.

The scanning electron microscopy (SEM) images, presented in Fig. 3 (a) and (b) visualize part of the sparse array and a single IR resonator within the sparse array, respectively. These images confirm the successful fabrication of the resonators and show their connection to the routing paths. Fig. 3 (a) shows the sparseness of the array and the advantageous routing, and in Fig. 3 (b) an image of a device at the pixel level can be seen together with several parallel routing lines (to the right). The innovative approach in creating this array demonstrates its potential for high-resolution thermal imaging in environments previously deemed too hostile for such technology.

CHARACTERIZATION AND RESULTS

The IR response of the devices has been evaluated at JPL and Stanford using a temperature-controlled probe station across various temperatures up to 500°C. Characterization of the fabricated arrays was done through microwave measurements, using RF probes connected to a Vector Network Analyzer (VNA). Each pixel was measured and evaluated, revealing clear resonant peaks with Q-factor ~2000, calculated using the frequency-to-3dB bandwidth ratio of the resonator.

Measurements of several resonators indicated a consistent and reliable operation across the entire array. Figure 4 (a) shows a typical resonator performance at room temperature without any IR source present. The S_{21} parameter was obtained over a span of approximately 500 MHz. The first, second and third resonance peaks can be clearly seen. The insert in Fig. 4 (b) shows a photo taken through the optical microscope showing one of the RF probes measuring a device.

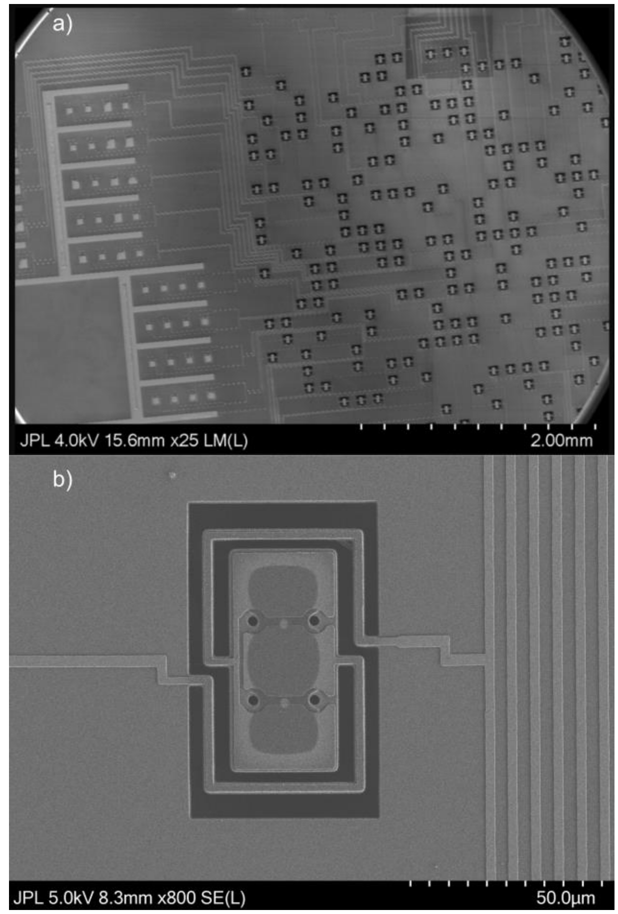

Figure 3: (a) A SEM image of parts of the sparse array, and (b) a zoomed in single S-designed IR resonator, where routing paths are visible to the right.

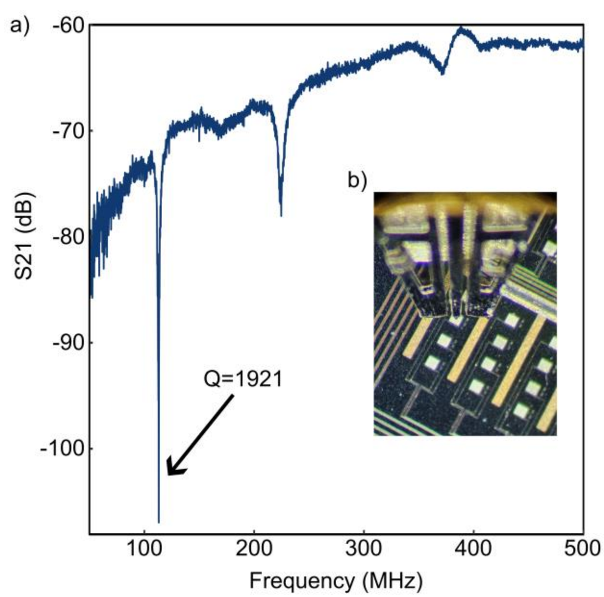

Figure 4: (a) S_{21} as a function of frequency of one resonator, measured at room temperature, using (b) an RF probe.

Additional rigorous evaluations were done under extreme conditions which involved subjecting the array to a broad temperature range, spanning from room temperature (RT) to 490°C. A specific cooling system was utilized for the probes for preserving purposes and the sample was held on a temperature stage, as depicted in Fig. 5. The data was obtained using a VNA. This same set-up was used for IR measurements, explained and presented further, later on in the paper.

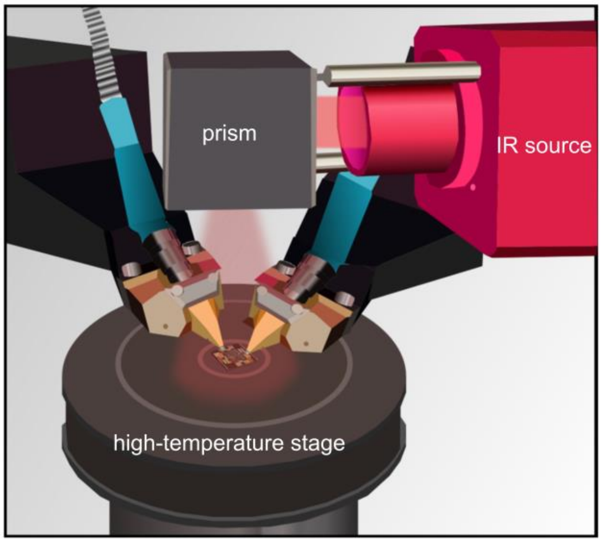

Figure 5: Schematic image of the high-temperature measurement setup with the chip under exposure from the IR source, where the light was directed with a prism.

This high-temperature testing regimen entailed monitoring the resonant frequency shifts of individual pixels within the array when exposed to elevated temperatures. The obtained high-temperature data is shown in Fig. 6 (a) demonstrating these shifts. The S_{11} parameter was studied for a high-order resonant frequency at 910 MHz while increasing the temperature in regular increments. The data shows that both a change in amplitude and resonant frequency can be visually observed. A clear linear relationship could be obtained between the temperature increase and the resonant frequency, up to 490°C, as presented in Fig. 6 (b) – a notable departure from traditional IR detectors prone to saturation at significantly lower temperatures [15].

Additional measurements were conducted with the device illuminated by an IR source, as depicted in Figure 7. These measurements capture the resonant response of the array at 490°C, both with and without the IR lamp activated, as can be seen in Fig. 7. Activation of the IR signal results in a discernible shift in resonant frequency, indicating the device's responsiveness to incident IR power (red = IR lamp ON, black = IR lamp OFF). The resonant frequency shifts down by ~0.9 MHz. The estimated incident IR power is ~60 nW per pixel for a pixel size of 30 µm by 50 µm. The responsivity is, therefore, 16.3 ppm/nW of IR power.

DISCUSSION

By using compressed sensing-based methods, existing reconstruction algorithms, and toolboxes for reducing the sampling time of a high-resolution sensor array system, successful image recovery has been shown [16]-[18].

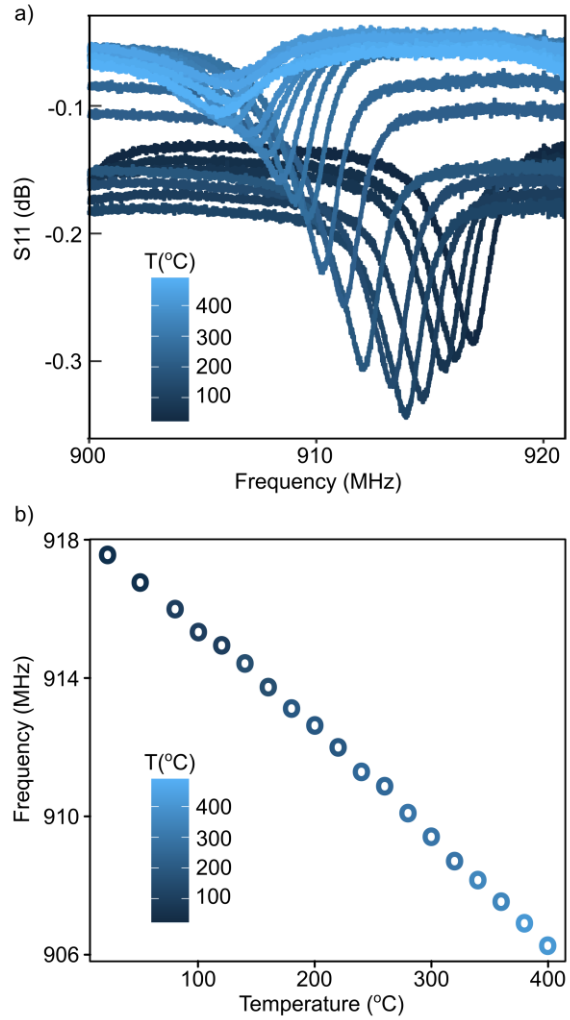

Figure 6: (a) S_{11} as a function of frequency measured at room temperature up to 490°C. (b) Linear temperature dependence in frequency shift as a function of temperature

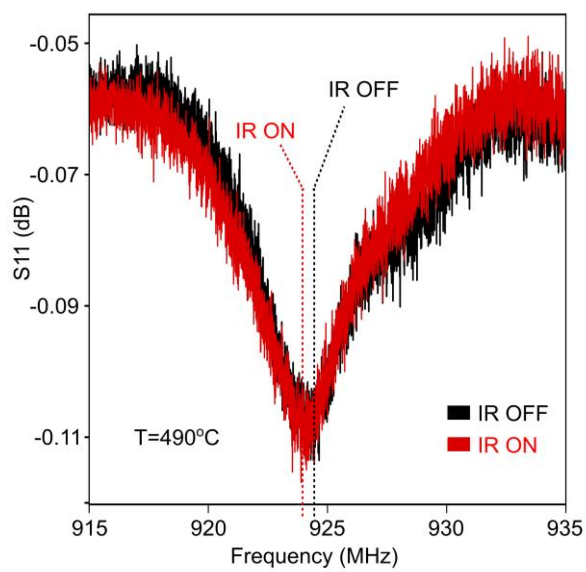

Figure 7: Frequency shift in the resonance frequency with (red) and without (black) IR exposure, at 490°C.

The reconstruction algorithm has been tested in prior simulations using a 128 by 128 resonator array with a density of 37.5% [1]. To assess the data recovery performance of the sparse array, a test image was used featuring intricate details and abrupt data changes (see Fig. 8). The performance metrics for this case are as follows: a correlation coefficient of 0.9785 and a recovery error of 0.08. These results suggest that small details are discernible, and the correlation coefficient is sufficiently high. It is worth noting that various random sparse array layouts with the same density are possible. Through experiments using 10 different arrays with identical densities, consistently high correlation coefficients were observed for densities exceeding 30%.

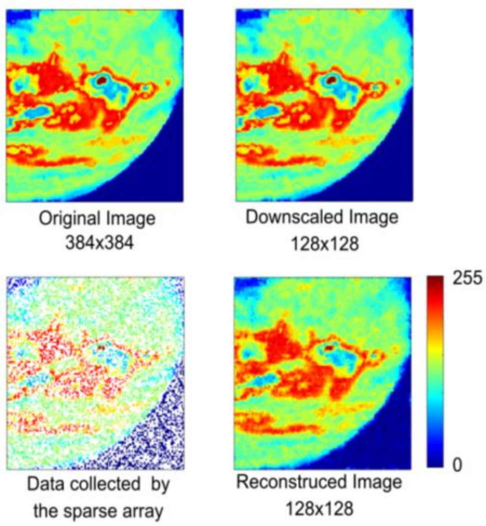

Figure 8: Image reconstruction using the designed random sparse arrays with the density of 37.5% [1]. (Original Image Credit: NASA/JPL-Caltech.)

CONCLUSION

In this paper, we presented measurement data of a new resonant thermal IR detector operating at 490 °C. The preliminary findings of this research not only validate the fabrication and functionality of these high-temperature resonant sensors but also lay the groundwork for future exploration of high-temperature planetary surfaces. The adaptability of this technology to various IR wavelengths, coupled with its potential scalability for larger arrays, heralds new possibilities for planetary science and remote sensing in the most inhospitable of environments.

ACKNOWLEDGEMENTS

This research was carried out at Jet Propulsion Laboratory, California Institute of Technology, under a contract with NASA (80NM0018D0004).

REFERENCES

[1] M. B. Coskun and M. Rais-Zadeh, 1. "Thermal Infrared Detector Sparse Array for NASA Planetary Applications," *5th IEEE Electron Devices Technology & Manufacturing Conference (EDTM)*, (2021).

[2] V.J. Gokhale and M. Rais-Zadeh, "Uncooled infrared detectors using gallium nitride on silicon micromechanical resonators," *JMEMS* 23 (4), pp. 803-810, 2014.

[3] P. Ephrat, L. Keenliside, A. Seabrook, F. S. Prato, J. J. L. Carson, "Three-dimensional photoacoustic imaging by sparse-array detection and iterative image reconstruction.," *J Biomed Opt*. 2008 Oct; 13(5): 054052. doi: 10.1117/1.2992131

[4] E. Roux et al., "2-D Ultrasound Sparse Arrays Multidepth Radiation Optimization Using Simulated Annealing and Spiral-Array Inspired Energy Functions," *IEEE Transactions on Ultrasonics, Ferroelectrics, and Frequency control*, Vol. 63, No. 12, Dec 2016.

[5] B. Diarraa, H. Liebgott, P. Tortoli and C. Cachard, "Sparse array techniques for 2D array ultrasound imaging," *Acoustics*, 2012.

[6] P. K. Weber, R. M. Schmitt, B. D. Tylkowski, et J. Steck, "Optimization of random sparse 2-D transducer arrays for 3-D electronic beam steering and focusing," *Proceedings of IEEE Ultrasonics Symposium*, Cannes, France, 1994, vol. 3, p. 1503-1506.

[7] B. Oreper, A. D. Foland, "X-ray imager with sparse detector array," US Patent 9069092 B2.

[8] D. Russomanno, S. Chari, and C. Halford, "Sparse Detector Imaging Sensor with Two-Class Silhouette Classification," *Sensors* 2008, 8, 7996-8015; DOI: 10.3390/s8127996

[9] J. R. Fienup, and P. S. Idell, "Imaging correlography with sparse arrays of electrodes," *Optical Engineering*, Vol. 27 No. 9, Sept.1988.

[10] P.Yang , B. Chen, K.R. Shi, "A novel method to design sparse linear arrays for ultrasonic phased array," *Ultrasonics*, 44 (2006) e717–e721.

[11]http://kiss.caltech.edu/study/venus/2015_KISS_Venus_Final_Report.pdf

[12] C. Chapin, R. Miller, K. Dowling, R. Chen and D.G. Senesky, "InAlN/GaN High Electron Mobility Micro-Pressure Sensor for High-Temperature Environments," *Sensors and Actuators A: Physical*, Vol. 263, pp. 216-223, Aug. 2017.

[13] M. Hou and D. G. Senesky, "Operation of ohmic Ti/Al/Pt/Au multilayer contacts to GaN up to 600°C in air," *Appl. Phys. Lett.*, vol. 105, no. 8, pp. 081905.1–081905.4, 2014.

[14] M. Ghatge, M. Rais-Zadeh and R. Tabrizian, "High- Q Gallium Nitride Thickness-Shear Baw Resonators with Reduced Temperature Sensitivity," *21st International Conference on Solid-State Sensors, Actuators and Microsystems (Transducers),* Orlando, FL, USA, 2021, pp. 1400-1403, doi: 10.1109/Transducers50396.2021.9495432.

[15] R. G. Azevedo et al., 1. "A SiC MEMS Resonant Strain Sensor for Harsh Environment Applications," *IEEE Sensors Journal*, vol. 7, no. 4, pp. 568-576, (2007).

[16] S. Wu et al., "Learning a compressed sensing measurement matrix via gradient unrolling," in *Proc. Int. Conf. Mach. Learn.*, 2019

[17] C. Sun, W. Li and W. Chen, "A Compressed Sensing Based Method for Reducing the Sampling Time of A High Resolution Pressure Sensor Array System," *Sensors*, 17(8):1848, 2017.

[18] Candes, E. J., and J. K. Romberg. "The l1 magic toolbox." (2006).

CONTACT

*I.H. Rodrigues, tel: +1-626-659-3017; rodrigues@jpl.nasa.gov
*M. Rais-Zadeh; email: Mina.Rais-Zadeh@jpl.nasa.gov